Computational optimisation of the acoustic performance of mufflers for sleep apnoea devices

Peter Jones and Nicole Kessissoglou

School of Mechanical and Manufacturing Engineering, The University of New South Wales, Sydney, Australia

ABSTRACT

Computational optimisation techniques are applied to maximise the acoustic performance of mufflers used in sleep apnoea devices. The mufflers are small and irregularly shaped, and as such their compact nature introduces complexities in the optimisation problem. A continuous positive airway pressure (CPAP) muffler comprising three inter-connected chambers was examined, with and without the presence of foam. The optimisation process involved development of an integrated model to couple the genetic algorithm function within Matlab with an acoustic finite element model of the muffler developed in COMSOL, with an objective to minimise the transmission loss of the muffler. Optimisation of the geometry of the CPAP device muffler in the absence of foam was initially performed. The inclusion of foam was then considered and optimisation of the foam dimensions at various frequency ranges was conducted. Results are compared with the transmission loss of the CPAP device muffler for which the reactive and resistive components were simultaneously optimised.

INTRODUCTION

Obstructive sleep apnoea (OSA) is a medical condition whereby the smooth muscles of the upper airway lose sufficient condition during sleep that the airway becomes constricted, resulting in partial or complete obstruction of the airway (Thorpy, 1990). Sleep apnoea affects approximately 10% of the adult population and has strong links to stroke and heart failure, as well as a strong association with obesity and diabetes (Young, 2009). OSA can be successfully managed through the application of a positive pressure to the airway. This elevated airway pressure is delivered via a mask using a flow generator comprising power supply, motor, fan, humidifier and control circuitry. The most widely used flow generator configuration maintains a constant airway pressure throughout the breathing cycle and is referred to as a continuous positive airway pressure (CPAP) device. CPAP devices function by using a small motor/fan unit to produce the elevated airway pressure. The fans run at speeds up to 30,000 rpm and, because of the high and varying speed, generate noise which is annoying to the user and sleep partner.

Compliance with treatment for OSA is poor, with half of patients discontinuing therapy within the first year. A significant root cause identified for such low compliance is the noise emitted by the flow generating device (Stuart, 2010). Noise from the flow generator is controlled using mufflers situated in the air flow paths to and from the fan. The mufflers are very small, irregularly shaped and often consist of several interconnected volumes. While they are predominantly reactive, dissipative materials are often incorporated into the design to enhance the acoustic performance and to extend the attenuated frequency range up to 5 kHz.

This paper investigates optimisation of the acoustic performance of a muffler design found in a CPAP device. A finite element (FE) model of the muffler is developed to obtain its transmission loss. The acoustic characteristics of a polyurethane foam typically used as the dissipative material in CPAP device mufflers was experimentally measured, from which the equivalent fluid properties were obtained. These properties were then incorporated into the FE model of the CPAP device muffler design. Computational optimisation techniques were then applied to maximise the muffler acoustic performance. Optimisation of the muffler reactive geometry was initially examined. The inclusion of foam was then considered and optimisation of the foam dimensions was performed. Results are also obtained for the transmission loss of the CPAP device muffler for which the reactive and resistive components were simultaneously optimised.

CPAP DEVICE MUFFLER DESIGN

The design of the CPAP device muffler consists of three interconnected expansion chambers each having orthogonal inlet and outlet ports. The chambers are geometrically simple and contain no internal baffles. Figure 1 shows a diagram of the muffler with exaggerated lengths of the interconnecting ducts, and clearly shows the three chambers and inlet and outlet ports of each chamber. The actual muffler, shown in Fig. 2, is more compact. Eight dimensions are assigned as control variables (CV), indicated by red lines in Fig. 2, and are utilised in the optimisation process. A further two control variables are used to define the thickness of foam inserts which are located at the bottom of chambers 2 and 3.

The horizontal dimension of chamber 2 that is normal to CV5 is constrained to be equal to the diameter of chamber 1. The rear face of chamber 3 is co-planar with the axis of the inlet duct. The interconnecting duct between chambers 1 and 2 is located in the centre of the rectangular face at the outlet of chamber 1. The interconnecting duct between chambers 2 and 3 shares the same vertical offset from the top face as the previous duct and is offset horizontally from the front-most face by the distance CV6. The outlet duct shares the same vertical offset from the top face as the previous ducts and is located horizontally in the centre of the front-most face. Whilst the lengths of the interconnecting ducts can vary, the duct diameters remain fixed. Complex inter-relationships exist between the control variables and the underlying muffler geometry. Changing a variable attached to one component of the system has the potential to influence the

acoustic behaviour of other components by affecting expansion ratios, chamber volumes, and/or duct locations.

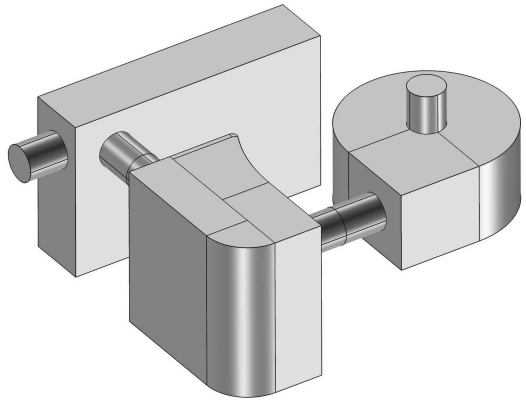

Figure 1. Design of the CPAP device muffler showing three interconnected chambers each having orthogonal inlet and outlet ports

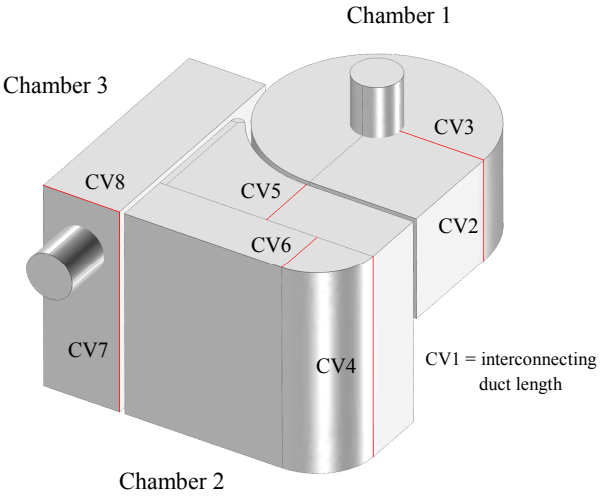

Figure 2. CPAP device muffler showing the control variables

FINITE ELEMENT MODELLING

A finite element model of the CPAP muffler geometry was developed using COMSOL (version 4.0a). The model was meshed using Lagrange-quadratic elements. A harmonic pressure of 1 Pa was specified at the muffler inlet and a high-order non-reflecting boundary condition was applied at the muffler inlet and muffler outlet. The calculation of transmission loss using non-reflecting boundary conditions produces a measure of performance which is an intrinsic property of the muffler. The actual performance of the muffler will be affected by the in-situ source and termination impedances.

Transmission loss was calculated directly in COMSOL using the acoustic power at the inlet and outlet of the acoustic system.

$$TL = -10\log_{10}\left(\frac{|P_t^2|}{|P_i^2|}\frac{S_{out}}{S_{in}}\right) \quad (1)$$

where P_i and P_t are respectively the pressures of the incident and transmitted waves, and S_{out}, S_{in} are respectively the cross sectional area of the pipes at the muffler inlet and outlet.

Mean flow was not included in the calculation of transmission loss as maximum airflow velocities likely to be encountered in sleep apnoea devices are less than Mach 0.02. Flow-acoustic interactions can generally be considered negligible below $M < 0.1$ (Ih and Lee, 1987).

CHARACTERISATION OF FOAM PROPERTIES

Equivalent fluid properties

Porous materials can be modelled using the equivalent fluid approach, in which the the material properties are represented by a complex speed of sound c_f and a complex mean density ρ_f by (Seybert *et al.*, 1998)

$$c_f = j\frac{\omega}{\gamma} \quad (2)$$

$$\rho_f = -j\frac{Z_c\gamma}{\omega} \quad (3)$$

Z_c is the characteristic impedance, γ is the propagation constant, ω is the radian frequency and $j = \sqrt{-1}$ is the imaginary unit.

The characteristic impedance and propagation constant can be obtained using the functions proposed by Delany and Bazley (1970). The Delany-Bazley functions can be expressed in terms of coefficients C_1 to C_8 by

$$Z_c = \rho_a c_a\left[1 + C_1\left(\frac{\rho_a f}{r_f}\right)^{C_2} - jC_3\left(\frac{\rho_a f}{r_f}\right)^{C_4}\right] \quad (4)$$

$$\gamma = \left(\frac{\omega}{c_a}\right)\left[C_5\left(\frac{\rho_a f}{r_f}\right)^{C_6} + j\left(1 + C_7\left(\frac{\rho_a f}{r_f}\right)^{C_8}\right)\right] \quad (5)$$

where ρ_a and c_a are respectively the density and speed of sound in air, f is the frequency in Hz and r_f is the airflow resistivity in MKS units. It is well known that the Delany-Bazley empirical relations are unable to encapsulate the acoustic behaviour of foams sufficiently to be regarded as universally applicable (Attenborough, 1986). Several authors have derived different sets of coefficients for poroelastic materials, however they are only relevant to the particular foam for which they were obtained (Mechel 1986; Miki 1990; Dunn and Davern 1986; Wu 1988).

Acoustic characterisation of foam properties can be obtained by experimentally obtaining the characteristic impedance Z_c, propagation constant γ and airflow resistivity r_f of the material and fitting the data to Eqs. (4) and (5) to obtain the unknown coefficients. However, whilst the equivalent fluid properties can be obtained from experimental measurement of Z_c, γ and r_f, the input data to a finite element model will not be continuous as they are sampled at discrete frequencies. Continuous data can be obtained by curve fitting the experimental data to the Delany and Bazley empirical functions given by Eqs. (4) and (5) using the non-dimensional normalising parameter $\rho_a f/r_f$.

Experimental Measurement of Foam Properties

The characteristic impedance and propagation constant of the polyurethane foam were measured using an impedance tube and applying the transfer function method to a two-cavity

approach as described by Utsuno *et al.* (1989). The airflow resistivity was measured according to the direct airflow method described in ISO 9053 (1991). The experiments are described in what follows.

For measurement of the characteristic impedance Z_c and propagation constant γ, a sample of the polyurethane foam of length d was positioned within a Brüel & Kjær Type 4206 impedance tube and against the front face of a moveable plunger. The plunger was then withdrawn away from the sample, producing an air cavity with a known air cavity depth L between the rear face of the sample and the plunger, as shown in Fig. 3. A random signal was fed to the loudspeaker of the impedance tube and the normal surface acoustic impedance of the sample was measured in accordance with ISO 10534 (1998). The transfer function H_{12} from microphone position 1 to position 2, defined by the complex ratio p_2/p_1, was measured using a two channel Fast Fourier transform. The surface acoustic impedance Z_0 is then obtained by (Munjal and Doige, 1990)

$$Z_0 = jZ_a\left(\frac{H_{12}\sin\big(k_a(L_x+D_x)\big)-\sin(k_aL_x)}{\cos(k_aL_x)-H_{12}\cos\big(k_a(L_x+D_x)\big)}\right) \tag{6}$$

where k_a is the wavenumber of air and Z_a $(=\rho_a c_a)$ is the characteristic impedance of air. The impedance tube plunger was withdrawn a further distance and the measurement procedure was repeated at depth L' to obtain Z_0'. The theoretical impedance of closed tubes with depths L and L' is given by (Utsuno *et al*., 1989)

$$Z_1 = -jZ_a\cot(k_aL)\,, \qquad Z_1' = -jZ_a\cot\big(k_aL'\big) \tag{7}$$

The characteristic impedance Z_c and propagation constant γ of the material can then be calculated by (Utsuno *et al*., 1989)

$$Z_c = \pm\sqrt{\frac{Z_0Z_0'(Z_1-Z_1')-Z_1Z_1'(Z_0-Z_0')}{(Z_1-Z_1')-(Z_0-Z_0')}} \tag{8}$$

$$\gamma = \left(\frac{1}{2d}\right)\ln\left(\left(\frac{Z_0+Z_c}{Z_0-Z_c}\right)\left(\frac{Z_1-Z_c}{Z_1+Z_c}\right)\right) \tag{9}$$

where the sign in Eq. (8) is selected so that the real part of Z_c is positive.

The airflow resistivity of a homogeneous material is given by $r_f = \Delta P/du$, where ΔP is the static pressure drop across the material, d is the unit thickness and u is the linear velocity of air passing through it (ISO 9053:1991). Airflow resistivity for the polyurethane foam was measured according to the direct airflow method described in ISO 9053 (1991). A unidirectional airflow was passed through a cylindrical sample of 25 mm thickness and 100 mm diameter and the resulting pressure drop between the two free faces of the sample was measured. A schematic diagram of the airflow resistivity experimental rig is shown in Fig. 4.

The experimentally measured characteristic impedance Z_c, propagation constant γ and airflow resistivity r_f were then curve fitted to Eqs. (4) and (5) to obtain the unknown coefficients C_1 to C_8. Equations (2) and (3) were then used to obtain the complex speed of sound and complex density of the polyurethane foam. These equivalent fluid properties were then incorporated into the FE model of the muffler developed in COMSOL.

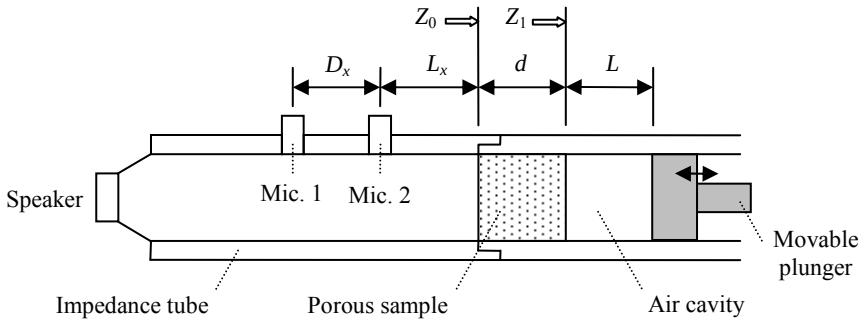

Figure 3. Schematic diagram of the impedance tube configuration

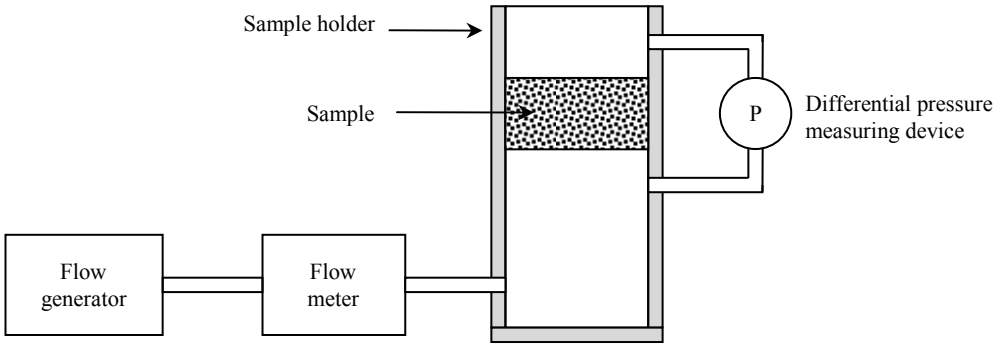

Figure 4. Schematic diagram of the airflow resistivity experimental set-up

OPTIMISATION

Optimisation Procedure

Optimisation was performed using a combination of the COMSOL and MATLAB software packages and made use of the former's ability to write out the finite element (FE) analysis database as a MATLAB compatible m-file. Three scripts, titled Input, Objective Function, and Optimisation Algorithm, control the optimisation process as follows. The Input script contains all of the variables that are required to define the optimisation problem and includes:

- the frequencies to be considered;
- the relative weighting to be placed on the objective function calculated at each frequency; and
- the initial values and bounds to be applied to each of the control variables.

The script also defines the convergence criteria to be applied to the optimisation. Control is passed to the second script which, on completion, returns the optimised value of the objective function and the corresponding control variable values. The original script writes out the data and terminates. The Objective Function script comprises two functions linked by an iterative process. The first function calls the optimisation algorithm which is contained in the external Optimisation Algorithm script. The optimisation algorithm used in this work is the genetic algorithm function within MATLAB. The genetic algorithm (GA) optimisation script then calls the second function to perform the FE analysis and return objective function values. The process performed by the Optimisation Algorithm script is iterative until an optimised solution has been obtained.

Transmission loss was used as the objective function to minimise. Optimisation of the transmission loss averaged across multiple frequencies is described by

$$f_o(\boldsymbol{x}) = \sum_{k=1}^{q} \varphi_k \; TL(\boldsymbol{x}, f_k)\,, \qquad \sum_{k=1}^{q} \varphi_k = 1 \tag{10}$$

where f_o is the objective function. The vector $\boldsymbol{x} = [\mathrm{CV}_1, \ldots, \mathrm{CV}_n]$ contains the control variables, CV, that are used to define the geometry of the muffler components. The vectors $\boldsymbol{f} = [f_1, \ldots, f_q]$ and $\boldsymbol{\varphi} = [\varphi_1, \ldots, \varphi_q]$ contain the frequencies in the range being evaluated and the fractional weighting applied to the transmission loss at each frequency, respectively. q is the number of frequencies being evaluated and n is the number of control variables. The optimisation was based on the averaging the intrinsic transmission loss of the muffler at each frequency. This approach is consistent with that taken by Lee and Kim (2009) and Airaksinen and Heikkola (2010). An alternative approach would have been to combine the transmission loss of the muffler design with the sound power spectrum of the noise source and optimise the design based on minimising the average attenuated sound power.

The acoustic FE model was prepared within the COMSOL graphical user environment, taking care to define the control variable dimensions and frequency range as named variables. The database was then exported as a MATLAB m-file. Minor changes were made to the m-file to convert it into a function and to modify the dimension, frequency and output variable statements to facilitate exchange of data with the Objective Function and Optimisation Algorithm scripts. The resulting code was embedded into the Objective Function script as the second function.

Control Variables of the CPAP Device Muffler

A range of optimisation analyses were applied to the three-chamber CPAP device muffler shown in Fig. 2. Table 1 presents the dimensions of the pre-optimised (original) CPAP muffler design, as well as the lower and upper bounds placed on the ten control variables during the optimisation analyses. The upper bounds for the two control variables which are used to define the foam thickness at the bottom of chamber 2 and chamber 3 are not fixed values. Instead, these bounds are described in terms of the difference between the height of chamber 1 (CV2) and the height of the chamber containing the foam insert (CV4 and CV7 for chambers 2 and 3, respectively). As any, or all, of these chamber heights may be permitted to vary during the optimisation process, the upper bounds on the foam thickness will also change. The foam constraints are illustrated in Fig. 5.

Table 1. Pre-optimisation dimensions and bounds of the optimisation control variables

Control variable	Pre-optimisation dimension (mm)	Lower bound (mm)	Upper bound (mm)
CV1	2	2	10
CV2	40	30	60
CV3	84	60	100
CV4	80	45	100
CV5	25	10	45
CV6	44	30	55
CV7	80	45	100
CV8	30	30	50
CV9	NIL	5	CV4-CV2
CV10	NIL	5	CV7-CV2

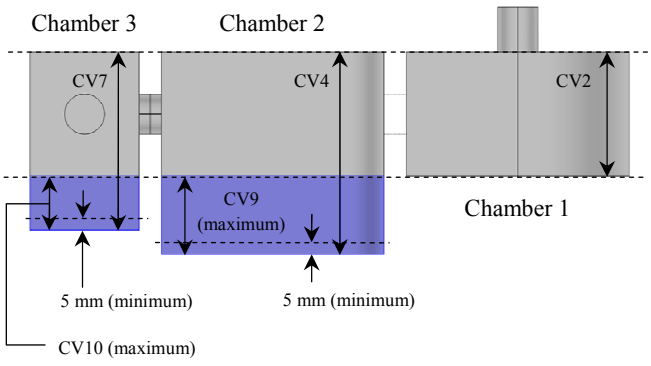

Figure 5. CPAP device muffler showing foam constraints

Noise Source Spectrum

To optimise the acoustic performance of the CPAP device muffler, the sound power spectrum of a known noise source was considered and the frequency bands where attenuation was desirable were considered. Figure 6 presents a noise source spectrum generated by the fan of a CPAP device for a frequency range up to 5 kHz. Beyond 5 kHz, the sound power level of the noise source decreases with increasing frequency and thus does not significantly contribute to the radiated noise. The noise spectrum clearly shows two frequency bands within this range to be targeted by the muffler. The first band extends from 500 to 1200 Hz and is centred on the low frequency peak at around 1 kHz. The second band is broader and spans the higher frequency region between 2 and 5 kHz. Attenuation in these two bands will be dominated by the reactive geometry and acoustically absorptive foam, respectively.

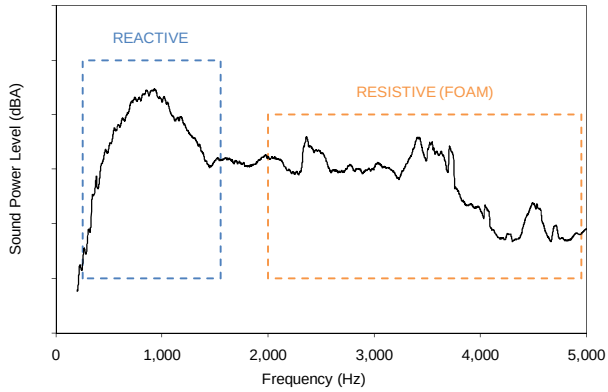

Figure 6. Sample CPAP fan noise source spectrum

The various optimisation analyses for the CPAP muffler are described in what follows. The reactive geometry of the muffler was initially optimised to attenuate the peak noise around 1 kHz in the lower frequency band. This geometry was then fixed and the resistive component of the muffler, corresponding to the two foam inserts, was optimised to attenuate the broadband noise at higher frequencies (2–5 kHz). A third optimisation was performed which simultaneously optimised the muffler geometry and the thickness of the foam inserts and included frequencies from both the lower and higher frequency bands. The transmission loss resulting from optimisation of the reactive and resistive muffler components separately is compared with the transmission loss obtained from the simultaneous optimisation run.

RESULTS

Transmission loss of pre-optimised muffler

Using the original dimensions of the muffler listed in Table 1, the transmission loss of the muffler with and without the presence of foam was calculated and the results are presented in Fig. 7. In the pre-optimised design, the foam inserts occupy the lower half of chambers 2 and 3. The transmission loss of the muffler in the absence of foam shows poor performance below 800 Hz and an uneven performance at higher frequencies. The inclusion of foam reduces the transmission loss peak at around 1 kHz but in general improves performance at higher frequencies.

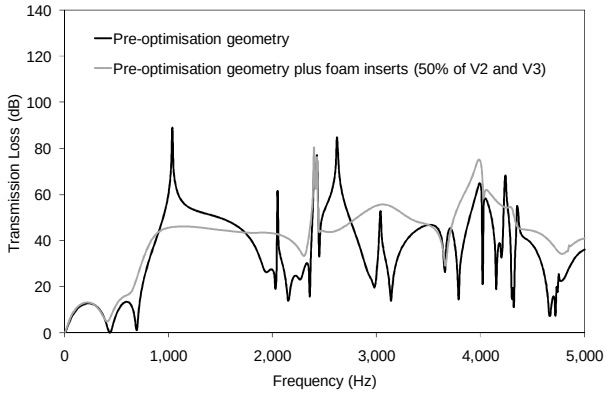

Figure 7. Transmission loss using the pre-optimised (original) geometry of the CPAP muffler – reactive muffler only (black line); with foam inserts occupying the lower half of chambers 2 and 3 (grey line)

Reative muffler geometry optimisation

Optimisation of the geometry of the reactive component of the CPAP device muffler was conducted considering eight equally weighted frequencies in the lower frequency band, from 500 to 1200 Hz in 100 Hz increments. The control variables CV1 to CV8 and the bounds shown in Table 1 were used. The pre-optimised (original) and optimised dimensions that were obtained using the genetic algorithm are presented in Table 2. Comparison of the optimised values with the lower and upper bounds in Table 1 shows that all optimised dimensions have increased yet only three of the eight dimensions are within 5 mm of their upper bound. Only the length of the interconnecting ducts has optimised to its upper bound value. Optimisation of the reactive muffler geometry results in an increase in the volume of each chamber and an increase in the expansion ratios.

Table 2. Original and optimised control variables for the reactive only optimisation of the CPAP muffler

Control variable (mm)	Original dimensions	Optimised dimensions
CV1	2	10
CV2	40	52
CV3	84	90
CV4	80	94
CV5	25	42
CV6	44	49
CV7	80	89
CV8	30	47
Averaged TL (0.5-1.2 kHz)	33.6 (dB)	62.5 (dB)
Averaged TL (entire 5 kHz range)	36.3 (dB)	54.9 (dB)

The transmission loss of the muffler in the absence of foam, using the original dimensions and using the optimised geometry, is shown in Fig. 8. The low frequency band from 500 to 1200 Hz over which the optimisation was carried out is also highlighted. Optimisation of the muffler geometry in the low frequency band has resulted in an increase in transmission loss in that frequency band, as well as a significant increase in transmission loss at higher frequencies.

Using the optimised geometry, foam was then inserted to occupy the lower half of chambers 2 and 3, as in the case for the results presented in Fig. 7. Comparison of Fig. 9 with Fig. 7 confirms that the presence of foam reduces the transmission loss peaks below 2 kHz, but results in a more uniform transmission loss across the higher frequency range. The averaged transmission loss across the entire 5 kHz frequency range for the pre- and post optimised muffler geometries with foam inserts included are 41.8 dB and 56.3 dB, respectively. Comparison of these two values and the results presented in Figs. 7 and 9 shows that optimisation of the muffler geometry alone has already produced a significant increase in transmission loss across the entire frequency range.

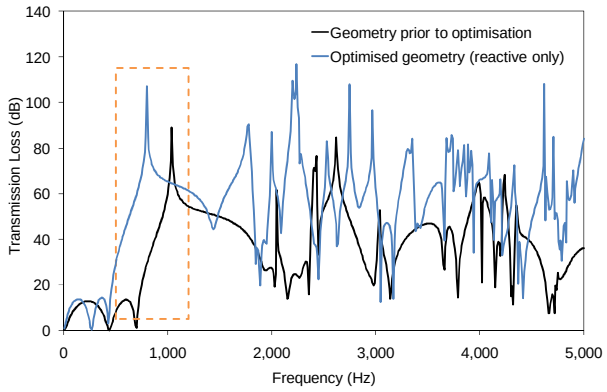

Figure 8. Transmission loss of the reactive CPAP muffler (no foam) – original dimensions (black line); optimised geometry (blue line)

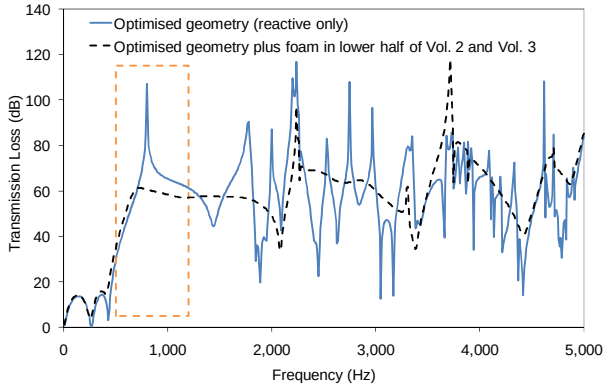

Figure 9. Transmission loss of the optimised CPAP muffler – reactive muffler only (blue line); with foam inserts in the lower half of chambers 2 and 3 (black dashed line)

Resistive muffler foam thickness optimisation

Using the optimised muffler geometry dimensions listed in Table 2, the thickness of the foam inserts located in chambers 2 and 3 were then optimised. Three frequency regions were considered – the low frequency band only (from 500 to 1200 Hz), the high frequency band only (from 2 to 5 kHz), and the low frequency and high frequency bands combined. During the foam optimisation, only the foam thickness in chambers 2 and 3 corresponding to control variables CV9 and CV10 was allowed to vary, that is, control variables CV1 to CV8 were fixed. A minimum foam thickness of 5 mm, as indicated by the lower bound in Table 1, was enforced in order to prevent the portion of either chamber occupied by foam from collapsing to zero volume and risking the generation of poor quality finite element mesh. Upper bounds were applied which allowed the foam inserts to extend up to the plane defined by the bottom surface of chamber 1. This ensured that chambers 2 and 3 always retain foam-free regions having a minimum height corresponding to the height of chamber 1.

Commencing with the low frequency band, optimisation was carried out across the eight equally spaced frequencies considered previously in the reactive muffler geometry optimisation, that is, from 500 to 1200 Hz in 100 Hz increments. The second optimisation run was performed across the high frequency band only and considered seven equally weighted frequencies from 2 to 5 kHz in 500 Hz increments. The third optimisation run was then conducted combining the narrow low frequency band with the broad high frequency band. Hence, a total of fifteen equally weighted frequencies were considered. The optimised foam thickness for chambers 2 and 3 obtained using the genetic algorithm are summarised in Table 3 and the resulting transmission loss curves are presented in Fig. 10.

Table 3 shows that optimisation performed in the low frequency band produces the greatest averaged transmission loss of the three optimisation runs for that frequency band. Similarly, optimisation in the high frequency band produces the greatest averaged transmission loss for that frequency band. Optimisation across both the low and high frequency bands produces similar averaged transmission loss values in the individual and combined frequency bands. Figure 10 shows that the transmission loss peak below 1 kHz is greatest when the thickness of the foam inserts is optimised in the low frequency band, and reduces as the optimisation shifts to the high frequency band. This is due to the fact that optimising the foam inserts in the low frequency band results in the smallest values for the foam thickness, thus increasing the effective resonant reactive volume. The decrease in performance of the muffler at frequencies up to 2 kHz when optimisation is carried out in the high frequency band is attributed to the increased thickness of foam in chambers 2 and 3. The best performance of the muffler across the entire frequency range occurs when the foam thickness optimisation is performed in the high frequency band (from 2 to 5 kHz). This is due to the presence of the foam inserts making the greatest positive contribution to the muffler transmission loss at higher frequencies while reducing performance at the lower frequencies to a lesser extent. Optimisation in the high frequency band produces the thickest foam inserts of the three optimisations performed, as shown in Table 3.

Table 3. Optimised foam thickness control variables for the CPAP muffler

	Frequency bands for foam optimisation		
Control variable (mm)	Low frequency band	High frequency band	Both frequency bands
CV9	34	42	41
CV10	5	30	16
Averaged TL (0.5–1.2 kHz)	59.9 (dB)	55.9 (dB)	57.7 (dB)
Averaged TL (2–5 kHz)	59.4 (dB)	63.3 (dB)	62.5 (dB)
Averaged TL (0.5-1.2 kHz and 2–5 kHz)	59.7 (dB)	59.4 (dB)	59.9 (dB)
Averaged TL (entire 5 kHz range)	55.7 (dB)	56.6 (dB)	56.2 (dB)

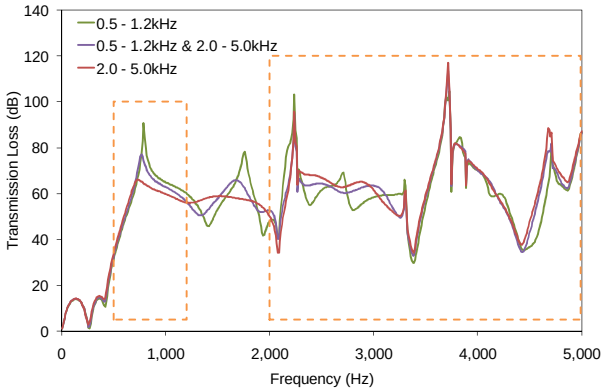

Figure 10. Transmission loss for resistive design optimisation of the CPAP device muffler in the low frequency band, high frequency band and combined low and high frequency bands

Simultaneous geometry and foam optimisation

Commencing with the pre-optimised (original) dimensions for the control variables listed in Table 1, the reactive muffler geometry and thickness of foam inserts located in chambers 2 and 3 of the prototype CPAP muffler were optimised simultaneously. All control variables (CV1 to CV10) were allowed to vary within their lower and upper bounds, also listed in Table 1. Optimisation was conducted considering the same fifteen equal weighted frequencies in the low and high frequency bands that were used earlier for the sequential reactive geometry and foam thickness optimisations.

The dimensions of the control variables obtained using the simultaneous geometry and foam optimisation in the low and high frequency bands are presented in Table 4, alongside those obtained by sequentially optimising the reactive geometry in the low frequency band and then optimising the foam thickness in the high frequency band. Comparison of the results obtained from the simultaneous and sequential optimisations shows both significant variation in the final designs and difference in the averaged transmission losses.

The averaged transmission loss across the entire frequency range of 62.2 dB and 56.6 dB for the simultaneously and sequentially optimised mufflers, respectively, shows that simultaneous optimisation of the reactive and resistive components of the muffler results in the best overall acoustic performance. Figure 11 compares the transmission loss for the simultaneous and sequential optimisations at the fifteen discrete frequencies in the low and high frequency bands. The simultaneous geometry and foam optimised design results in greater transmission loss in the low and high frequency ranges.

Table 4. Control variables for the sequential and simultaneous geometry and foam optimisation

Control variable (mm)	Sequential geometry then foam optimisation	Simultaneous geometry and foam optimisation
CV1	10	10
CV2	52	56
CV3	90	100
CV4	94	91
CV5	42	27
CV6	49	39
CV7	89	80
CV8	47	49
CV9	42	35
CV10	30	5
Averaged TL (entire 5 kHz range)	56.6 (dB)	62.2 (dB)

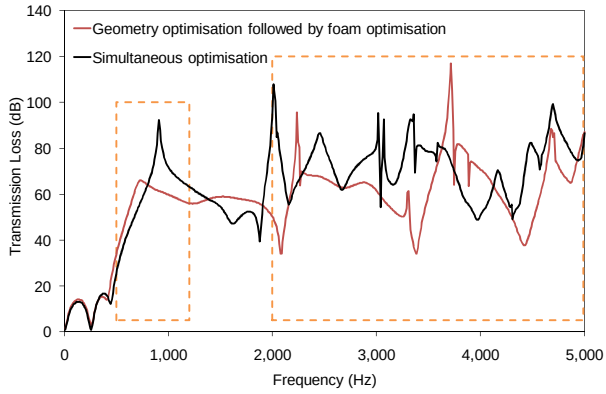

Figure 11. Transmission loss for sequential and simultaneous optimisation of the geometry and foam inserts of the CPAP device muffler

Table 5 presents a summary of the transmission loss results averaged over the entire 5 kHz frequency range for the various sequential and simultaneous optimisations of the CPAP device muffer. Also presented in Table 5 is the averaged transmission loss for the original (pre-optimised) geometry, and for the case when only the reactive muffler geometry is optimised and then foam is inserted into the

lower half of chambers 2 and 3. Optimisation of the muffler design has resulted in at least a 14 dB improvement in performance, as indicated by the averaged transmission loss across the entire frequency range, compared with that of the pre-optimised design. It was also shown that simultaneous optimisation of the muffler reactive geometry and thickness of foam inserts results in an improved performance in muffler acoustic performance, compared with the case when the reactive and resistive muffler components are sequentially optimised. In particular, simultaneous optimisation over both the low and high frequency bands yields a design having an averaged transmission loss for the entire frequency range which is 5.6 dB greater than that obtained by optimising the geometry in the low frequency band followed by optimising the foam in the high frequency band.

Table 5. Summary of averaged transmission loss across the entire 5 kHz frequency range for the various CPAP muffler design optimisations

Optimisation	Geometry	Foam	Averaged TL (dB)
NIL	Pre-optimisation	Fixed – Lower half of chambers 2 and 3	41.8
Geometry only	Low band[a]	Fixed – Lower half of chambers 2 and 3	56.3
Sequential - geometry followed by foam	Low band[a]	High band[b]	56.6
Simultaneous - geometry and foam	Both bands		62.2

[a]Low frequency band: 500 – 1200 Hz
[b]High frequency band: 2 – 5 kHz

CONCLUSIONS

In this work, computational optimisation techniques were used to maximise the acoustic performance of a CPAP device muffler. Optimisation of the complex reactive geometry as well as the amount of foam included within the muffler was performed. Optimisation in a low frequency band and a wider higher frequency band were conducted to take into account the sound power spectrum of the noise source. It was shown that optimisation of the muffler design has resulted in a significant improvement in performance across the entire frequency range considered. It was demonstrated that simultaneous optimisation of the muffler reactive geometry and thickness of foam inserts across the low and high frequency bands of interest resulted in an improved performance in muffler acoustic performance, compared with the case when the reactive and resistive muffler components were sequentially optimised.

ACKNOWLEDGEMENTS

Financial assistance for this work was provided as part of an ARC Linkage Project jointly funded by the Australian Research Council and ResMed.

REFERENCES

Attenborough, K. 1982, “Acoustical characteristics of porous materials”, *Physics Reports,* vol. 82, no. 3, pp. 179-227.

Delany, M.E. and Bazley, E.N. 1970, “Acoustical properties of fibrous absorbent materials”, *Applied Acoustics,* vol. 3, pp. 105-116.

Dunn, I.P. and Davern, W.A. 1986, “Calculation of acoustic impedance of multi-layer absorbers”, *Applied Acoustics,* vol. 19, pp. 321-334.

Ih, J.G. and Lee, B.H. 1987, “Theoretical prediction of the transmission loss of circular reversing chamber mufflers”, *Journal of Sound and Vibration*, vol. 112, pp261-272

ISO 9053:1991: *Acoustics – Materials for acoustical applications – Determination of airflow resistance*, International Organisation for Standardization, Switzerland.

ISO 10534-2:1998: *Acoustics – Determination of sound absorption coefficient and impedance in impedance tubes – Part 2: Transfer-function method*, International Organisation for Standardization, Switzerland.

Mechel, F.P. 1986, “Absorption cross section of absorber cylinders”, *Journal of Sound and Vibration*, vol. 107, pp. 131-148.

Miki, Y. 1990, “Acoustical properties of porous materials – Modifications of Delany-Bazley models”, *Journal of the Acoustical Society of Japan,* vol. 11, no. 1, pp. 19-28.

Munjal, M.L. and Doige, A.G. 1990, “The two-microphone method incorporating the effects of mean flow and acoustic damping”, *Journal of Sound and Vibration*, vol. 137, no. (1), pp. 135-138.

Seybert, A.F., Seman, R.A. and Lattuca, M.D. 1998, “Boundary element prediction of sound propagation in ducts containing bulk absorbing materials”, *Journal of Vibration and Acoustics – Transactions of the ASME*, vol. 120, pp. 976-981.

Stuart, M. 2010, “Sleep apnoea devices: The changing of the guard”, *Start-up*, vol. 15, no. 10, pp. 2-9.

Thorpy, M.J. (ed.) 1990, *International Classification of Sleep Disorders: Diagnostic and Coding Manual*, American Sleep Disorders Association, Minnesota, USA.

Utsuno, H., Tanaka, T., Fujikawa, T. and Seybert, A.F. 1989, “Transfer function method for measuring characteristic impedance and propagation constant of porous materials”, *Journal of the Acoustical Society of America*, vol. 86, no. (2), pp. 637-643.

Wu, Q. 1988, “Empirical relations between acoustical properties and flow resistivity of porous plastic open-cell foam”, *Applied Acoustics,* vol. 25, pp. 141-148.

Young, T. 2009, “Rationale, design, and findings from the Wisconsin Sleep Cohort Study: Toward understanding the total societal burden of sleep-disordered breathing”, *Journal of Clinical Sleep Medicine*, vol. 4, pp. 37-46.